Microfluidics and Nanofluidics (2019) 23:12
https://doi.org/10.1007/s10404-018-2172-z

RESEARCH PAPER

Facile fabrication of uniform nanoscale perfluorocarbon droplets as ultrasound contrast agents

Ruyuan Song[1] · Chuan Peng[3] · Xiaonan Xu[2] · Ruhai Zou[3] · Shuhuai Yao[1,2]

Received: 4 September 2018 / Accepted: 4 December 2018 / Published online: 5 January 2019

Abstract

Perfluorocarbon (PFC) nanodroplets have emerged as a novel phase-change contrast agent, remotely triggered by ultrasound in situ, which holds great potential for ultrasound imaging, early cancer diagnosis, and ultrasound-mediated cancer treatment. As the characteristics of PFC nanodroplets are highly size dependent, it is crucial to tightly control the size and uniformity of PFC nanodroplets, which remain a challenge using current available emulsification techniques. To meet this niche, we developed a novel method to produce monodisperse PFC nanodroplets by the Ouzo effect using a staggered herringbone micromixer. With this method, we fabricated PFC nanodroplets from ~ 200 to ~ 700 nm in diameter with a narrow size distribution (PDI < 0.1) and the throughput of nanodroplet production could be as high as 0.48 ml/h. The stability and biocompatibility of the prepared PFC nanodroplets were verified. Finally, the acoustic characterization of PFC nanodroplets was conducted to demonstrate the feasibility of PFC nanodroplets as ultrasound contrast agents via acoustic direct vaporization.

Keywords Microfluidic mixing · High throughput · Uniform PFC nanodroplets · Ultrasound imaging

1 Introduction

Ultrasound has been extensively employed in biomedical fields of diagnosis, therapy, and imaging-guided drug delivery during past 2 decades, in combination with lipid microbubbles of 1–8 μm in diameter as ultrasound contrast agents (Díaz-López et al. 2010a; Perera et al. 2015). However, microbubbles as the ultrasound imaging probes and drug carriers for ultrasound-mediate therapy have been hampered by their too large hydrodynamic diameter for effective extravasation into tumor tissues and poor stability (Perera et al. 2015). To address such limitations, phase-change perfluorocarbon (PFC) nanodroplets, made of perfluorocarbon oils with moderate boiling points such as perfluoropentane (PFP), perfluorohexane (PFH) or perfluorooctyl bromide (PFOB), have been developed to be the new-generation ultrasound contrast agents (Díaz-López et al. 2010b; Kaneda et al. 2009; Sheeran et al. 2012). Such PFC nanodroplets (typically ~ 200 nm) can pass through large inter-endothelial cell gaps (400–800 nm) of tumor vasculatures and accumulate in the tumor tissues, which makes it possible for ultrasound molecular imaging (Rapoport et al. 2007). The locally accumulated PFC nanodroplets are subsequently converted to be highly echogenic microbubbles by ultrasound activation in situ, which is called acoustic direct

This article is part of the topical collection "2018 International Conference of Microfluidics, Nanofluidics and Lab-on-a-Chip, Beijing, China" guest edited by Guoqing Hu, Ting Si and Zhaomiao Liu.

Electronic supplementary material The online version of this article (https://doi.org/10.1007/s10404-018-2172-z) contains supplementary material, which is available to authorized users.

✉ Ruhai Zou
zourh@sysucc.org.cn

✉ Shuhuai Yao
meshyao@ust.hk

[1] Bioengineering Graduate Program, Department of Chemical and Biological Engineering, The Hong Kong University of Science and Technology, Hong Kong, China

[2] Department of Mechanical and Aerospace Engineering, The Hong Kong University of Science and Technology, Hong Kong, China

[3] State Key Laboratory of Oncology in South China, Collaborative Innovation Center of Cancer Medicine, Department of Ultrasound, Sun Yat-sen University Cancer Center, Guangzhou, China

vaporization (ADV) (Reznik et al. 2011). Besides, ADV process can trigger the release of therapeutic cargos loaded in PFC nanodroplets and also facilitate the penetration and cellular uptakes of therapeutic agents (Rapoport et al. 2009b). The performance of PFC nanodroplets relies much more on the physical parameters (i.e., size and size distribution) than other nanoscale agents. Apart from size-dependent biological properties, such as circulation time and extravasation, the trigger frequency and the energy for PFC nanodroplets activation as well as the detection frequency for ultrasound imaging are tightly determined by the size of the nanodroplets (Reznik et al. 2011; Shpak et al. 2014). Besides, the vaporization of large ones in polydisperse PFC nanodroplets may cause gas embolism. Therefore, monodispersity of PFC nanodroplets is a critical measure. Unfortunately, conventional nanoemulsification techniques including high-shear stirring, sonication, high-pressure homogenization and membrane emulsification suffer from polydisperse populations of the fabricated nanodroplets, which fail to meet the demand of monodispersity of the PFC nanodroplets (Koroleva and Yurtov 2012).

In latest decades, the utilization of microfluidic systems to generate droplets has drawn substantial attention by virtue of its capacity to accurately control over the size, shape, and components of droplets. Monodisperse bubbles and droplets of a few microns in diameter have been manufactured as ultrasound contrast agents using microfluidics (Hettiarachchi et al. 2007; Martz et al. 2011; Segers et al. 2016; Talu et al. 2006). However, it is still fundamentally challenging to produce nanosized droplets in microfluidics, since nanoscale droplets are much smaller than the dimensions of typical microfluidic devices. Novel systems and strategies including step-emulsification (Shui et al. 2011), tip-steaming in hydrodynamic focusing (Jeong et al. 2012; Martz et al. 2012; Xu et al. 2017), condensation- and evaporation-assisted precursor synthesis (Seo and Matsuura 2014; Seo et al. 2015; Zhang et al. 2014), etc. have been developed to tackle this challenge. For example, step-emulsion requires one dimension of the channel compared to the formed nanodroplet size (Shui et al. 2011). Alternatively, Thomas Martz et al. produced PFC nanodroplets (360 ± 50 nm in diameter) via tip-streaming mode in a typical flow-focusing microfluidic device (Martz et al. 2012). However, the device was still very vulnerable to flow fluctuations operating in the tip-streaming mode. A few improvements such as three-dimensional flow-focusing (Jeong et al. 2012) geometries and axisymmetric co-flow (Xu et al. 2017) have been attempted to enhance the stability of droplet generation in the tip-streaming mode. Besides, Minseok Seo et al. obtained PFC nanodroplets condensed from gaseous PFC microbubbles, formed using a microfluidics device with heating elements at a temperature above the boiling point of the perfluorocarbon oil (Seo and Matsuura 2014). Similarly, precursor microdroplets may shrink into submicron droplets after the dissolution and evaporation of the volatile or water-soluble organic solvents (e.g., diethyl ether or ethanol) which were added into PFC oil prior to microfluidic emulsification (Seo and Matsuura 2014; Zhang et al. 2014). Nevertheless, the condensation method is limited for low-boiling point PFCs while the solvent evaporation method can only reduce the size by a limited factor. In addition to the prerequisite on the size controllability, throughput is another essential demand for the manufacturing of PFC nanodroplets for clinical applications (Lim et al. 2014). Unfortunately, all above-mentioned methods can only render a very low production rate.

Other than droplet generation by shear or flow focusing in microfluidic devices, nanodroplets can also be formed by a spontaneous emulsification effect, known as the Ouzo effect, in a ternary system (typically consisting of water, oil, and alcohol), where the oil dissolved in the alcohol precipitates out to form tiny droplets upon the addition of excessive water (Klossek et al. 2012; Vitale and Katz 2003). Unlike conventional emulsification methods, the Ouzo effect requires no mechanical agitation or addition of any surfactants, thus are more versatile for the synthesis of functional nanoemulsions (Kotta et al. 2012; Li et al. 2017), core–shell nanocapsules (Yan et al. 2014) and hollow fibers (Haase et al. 2015). Under the Ouzo effect, oil droplet nucleation is a rapid process at a timescale on the order of microseconds as a result of abrupt increase of the oil's supersaturation upon the addition of excess aqueous phase (Lu et al. 2017). To obtain homogeneous droplet nucleation that ensures a more uniform population of resultant droplets, ultrafast mixing between the two phases is required. Therefore, the size and size distribution of resultant oil droplets obtained by the Ouzo effect not only rely on the physicochemical properties and concentrations of the oil but also are highly relevant to the temporal and spatial characteristics of the mixing dynamics of the ternary system (Lepeltier et al. 2014; Zhang et al. 2015). Similar to oil droplet formation by the Ouzo effect, mixing of hydrophobic solutes (e.g., polymers and lipids) in a polar organic solvent with excess water has been extensively utilized to synthesize nanomaterials, which is commonly called nanoprecipitation or solvent shifting (Aschenbrenner et al. 2013; Beck-Broichsitter et al. 2015). Microfluidic mixers with mixing times at the millisecond scale have been demonstrated to control the size and size distribution of nanoparticles obtained from nanoprecipitation (Jahn et al. 2010; Karnik et al. 2008).

In this study, we demonstrate that uniform PFC nanodroplets are generated from a ternary system which consists of isopropanol (water–miscible solvent), perfluorocarbon oils (hydrophobic solute) and water (non-solvent) by the Ouzo effect in a high-throughput staggered herringbone mixer. The mixing time needs to be controlled at the millisecond scale to enable homogeneous nucleation of PFC oils. The

effects of flow parameters, PFC concentration, lipid concentration, and different kinds of PFC oils on the formation of PFC nanodroplets were investigated. The stability and biocompatibility of the synthesized PFC nanodroplets were verified. Finally, the synthesized PFC nanodroplets were acoustically converted to uniform echogenic microbubbles via a clinical ultrasound diagnostic system, and significantly positive contrast enhancement was present in the ultrasound images, proving that PFC nanodroplets could be used as ultrasound contrast agents.

2 Materials and methods

2.1 Materials

Ammonium persulfate, tetramethylethylenediamine (TEMED), perfluorooctyl bromide (PFOB), perfluorohexane (PFH), perfluoropentane (PFP) and isopropanol (IPA) were purchased from Sigma-Aldrich (St. Louis, MO, USA). Poly(dimethylsiloxane) (PDMS) (Sylgard 184) was purchased from Dow Corning (USA). 30% acrylamide/bis 29:1 solution was purchased from Bio-Rad (Hercules, CA, USA). Deionized water (Millipore Milli-Q grade) with resistivity of 18.0 MΩ·cm was used in all experiments. 1,2-Dipalmitoyl-sn-glycero-3-phosphocholine (DPPC), 1,2-distearoyl-sng-lycero-3-phosphoethanolamine-*N*-[methoxy(polyethylene glycol)-2000] (DSPE-PEG2000), and cholesterol were purchased from Avanti Polar Lipids (USA). MEM medium, fetal bovine serum, penicillin–streptomycin, 1,1′-dioctadecyl-3,3,3′,3′-tetramethylindocarbo-cyanine perchlo-rate (Dil), and fluorescein isothiocyanate (FITC) were purchased from Thermo Fisher Scientific (USA). Cell Counting Kit-8 was purchased from Dojindo Molecular (Japan).

2.2 Bulk synthesis of PFC nanodroplets

The IPA solution containing PFC oils at concentrations varying from 10 to 100 µl/ml was added into water, with organic/aqueous volume ratios varying from 1:100 to 20:100 under the magnetic stirring at 500 rpm. The stirring was kept for 10 min, allowing the system equilibrium for the PFC nanodroplet formation in water under constant mixing.

2.3 Microfluidics device fabrication and operation

We employed the staggered herringbone micromixer (Stroock et al. 2002) as the mixing device for the PFC nanodroplet fabrication. The staggered herringbone micromixer device consists of a 200-µm-wide and 70-µm-high channel, on the roof of which is patterned with 30-µm-high and 50-µm-thick herringbone features, as shown in Fig. 1a. The staggered herringbone micromixer was fabricated using the standard soft-lithography. Briefly, the designed patterns on a

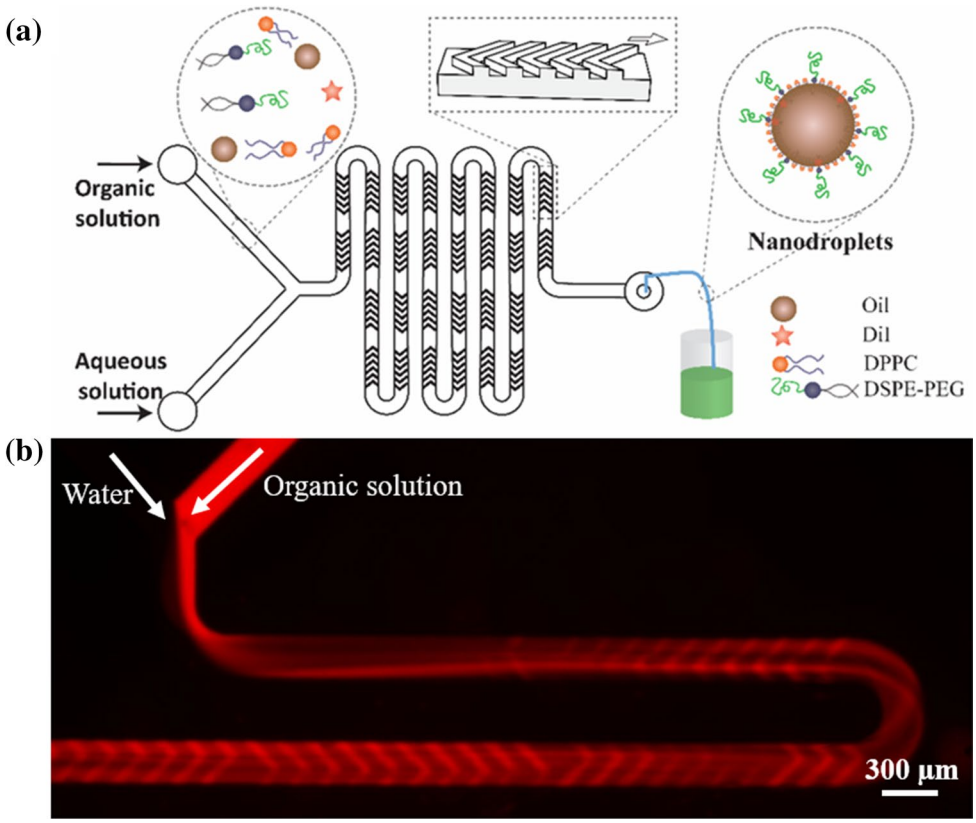

Fig. 1 **a** Illustration of the fabrication process of PFC nanodroplets by the Ouzo effect using the staggered herringbone mixer. The organic phase is an IPA solution with dissolved lipid mixture (i.e., DPPC, DSPE-PEG), PFC oil, and Dil. Dil is a red fluorescent dye for tracing the organic phase. **b** A fluorescent image showing the mixing process in the staggered herringbone mixer

photomask were transferred on a SU-8-coated silicon wafer by UV exposure and developed to obtain a SU-8 mold. A degassed PDMS mixture of base polymer and curing agent at mass ratio of 10:1 was poured over the SU-8 mold and cured at 80 °C for 2 h. Then resultant PDMS replica with punched access holes and clean glass slides were treated with O_2 plasma and bonded together. An IPA solution containing 1 mg/ml of lipid mixture, 5 µl/ml PFC oil and 5 µg/ml Dil was prepared as the organic solution. The lipid mixture includes DPPC, cholesterol, DSPE-PEG (2000) at a molar ratio of 8:4:1.2. The organic and aqueous solutions were pumped into the staggered herringbone micromixer using a syringe pump at a volume ratio of 1:4 and a total flow rate was 2 ml/min. The produced nanodroplets were collected at the outlet of the device. Subsequently, the samples were dialyzed against dd-H_2O to remove the organic solvent and concentrated by use of Amicon Ultra-15 centrifugal filter units (MWCO: 50 kD, Millipore).

2.4 Microfluidic device characterization

The mixing performance was quantitatively examined by fluorescence microscopy. The central fluid of 40 nM fluorescein isothiocyanate (FITC) was mixed with pure water from two side channels at different flow rates. The fluorescence images of the mixing flows were recorded using a microscope (Eclipse Ti-U, Nikon, Japan) equipped with a high-sensitivity video camera (Andor, Oxford Instrument, UK). The mixing time was estimated by calculating the time based on the travelling distance and the average flow rate of the fluid in the mixing channel.

2.5 Characterization of PFC nanodroplets

The size of PFC nanodroplets was characterized by dynamic light scattering (DLS) and transmission electron microscopy (TEM). For DLS measurement, a cuvette of 200 µL nanodroplet sample was measured by ZetaPlus analyzer (Brookhaven, USA) at a scattering angle of 90° for three times. For TEM imaging, 3 µl of nanodroplet solution was deposited on a copper grid, negatively stained with 1% wt/v phosphotungstic acid, and then examined by TEM (JEM 100CXII, JEOL, Japan) at 100 kV.

2.6 Cytotoxicity assay

The biocompatibility of PFC nanodroplets was evaluated on Hela cells. Hela cells were cultured with MEM medium supplemented with 10% fetal bovine serum and penicillin–streptomycin (100 U/ml) in a humidified atmosphere with 5% CO_2 at 37 °C. 100 µL of Hela cell suspension (~ 60,000 cells/ml) was added into each well of a 96-well plate and cultured overnight. Subsequently, the medium was replaced with 100 µL of fresh medium containing PFC nanodroplets of different concentrations and then cells were cultured for another 24 h. Then, the medium was replaced with 100 µL of fresh medium containing 10 µL Cell Counting Kit-8 (CCK-8, Dojindo, Japan) and the cells were incubated for 4 h. Finally, the absorbance of each well in the 96-well plate was measured by a multimode microplate reader (Varioskan LUX, Thermo Fisher, USA) at 450 nm to assess the cell viability.

2.7 In vitro ultrasound imaging

In vitro ultrasound characterization of PFC nanodroplets was performed in a polyacrylamide (PAA) hydrogel phantom. The PAA gel mixture was prepared with acrylamide solution (1.16 mL), 1.5 M Tris buffer (pH 8.8, 1.25 mL), ammonium persulfate solution (50 µL), and TEMED (5 µL). 2.5 mL of PFC nanodroplet suspension (5 µl/ml) was added into the prepared mixture and mixed gently to avoid bubble formation. The final mixture was immediately infused into a 5-ml thin-wall plastic Pasteur tube. The PFC nanodroplets were immobilized upon the gelation of acrylamide after approximately 1 h at room temperature and then stored at 4 °C before use. The ultrasound images of the PFC nanodroplets in the PAA gel were acquired by an ultrasound diagnosis system (Acuson S2000, Siemens, Germany). The plastic Pasteur tubes with the gel phantom were immersed into the water tank at 37 °C, at a distance of 2 cm away from the ultrasound transducer. The frequency of the transducer was fixed at 8 MHz. The activation of PFC nanodroplets was driven by 10-s high-intensity ultrasound at a mechanical index (MI) of 1.5, and the ultrasound images were taken at low-pressure ultrasound at an MI of 0.2 in the harmonic imaging mode.

2.8 Statistical analysis

Results were statistically analyzed using OriginPro 2016 and presented as mean ± standard deviation. The variance analysis and a two-tailed Student's t test were performed between two groups. A p value ($^{*}p < 0.05$) was considered to be statistically significant and a p value ($^{\#}p \geq 0.05$) was considered to be not statistically significant.

3 Results and discussion

3.1 Production of PFC nanodroplets

We examined the formation of nanodroplets in a PFOB–IPA–water ternary system. PFOB nanodroplets were formed by the nucleation of PFOB in IPA solution in response to a sudden increase in the oversaturation as a

consequence of the addition of water. Because PFOB and water are both miscible with IPA while PFOB is immiscible with water, the addition of water into the PFOB and IPA mixture leads to the spontaneous formation of tiny PFOB droplets. Their size is determined by the ratio of the components in the system (Vitale and Katz 2003). To obtain stable droplets in the nanoscale, we first identified the stable Ouzo region of the ternary PFOB–IPA–water phase by changing the concentration of PFOB in IPA and mixing ratio of IPA solution with water. The resultant droplets with diameter smaller than 1 μm were characterized as stable nanodroplets while unstable nanodroplets would aggregate to larger ones of over 1 μm in diameter (Yan et al. 2014). Figure S1 presents the narrow metastable region of the ternary PFOB–IPA–water phase diagram. When the weigh fraction of PFOB exceeded 0.01, large droplets (greater than 1 μm in diameter) were present in the droplet dispersions.

After setting the mixing ratio of the ternary system to ensure the stable nanodroplet formation, we need to initiate the Ouzo effect by a rapid process which leads to a uniform mixing of the PFOB/IPA and water. We performed the mixing process using a staggered herringbone micromixer. In the mixer, the organic solution and aqueous solution were injected from two side channels, respectively, and rapidly mixed when passing through a series of herringbone structures, as shown in Fig. 1b. In the organic phase, a mixture of lipids and PFOB was dissolved in the IPA solution. The hydrophobic PFOB solutes became supersaturated immediately and the PFC nanodroplets were formed by nucleation and subsequent growth. And the lipid molecules were absorbed on the surface of the PFOB nanodroplets to enhance the stabilization as well as to render excellent biocompatibility. The samples were collected from the outlet stream of the mixer and imaged by TEM. Spherical nanodroplets in the range of 190–250 nm were observed in the TEM image, as shown in Fig. 2a. Size measurement by DLS reported a mean diameter of 222.5 ± 10.7 nm and a narrow size distribution of 0.08 ± 0.03 in PDI. In comparison, the PFOB droplets prepared by magnetic stirring at the same PFOB concentration and organic/aqueous phase mixing ratio (MR), however, showed a bimodal distribution of nanodroplets with two peaks at 210 nm and 700 nm, respectively. The mean size was 382.4 ± 35.3 nm with a PDI of 0.22 ± 0.08, much larger in size and broader in size distribution than those produced by microfluidic mixing (Fig. 2b). We anticipate that, in the bulk stirring, the formed droplets may possess a W/O/W double emulsion structure with tiny water droplets in the center of oil droplets due to slow mixing, as illustrated in Fig. 3. Such phenomenon has also been observed in oil microdroplets where tiny water droplets were formed by nucleation of the water molecules dissolved in oil droplets during the evaporation and dissolution of a water–alcohol solution dissolved with oil (Tan et al. 2016).

We further investigated the effect of the mixing time on the PFOB nanodroplet size by changing the total flow rate in the mixer. The mixing time of the staggered herringbone micromixer decreased from ~47 milliseconds to ~2 milliseconds as the increase of the total flow rate from 0.2 to 4 ml/min (Fig. S2). The mean diameter of the PFOB nanodroplets decreased with the increase of the total flow rate (Fig. 4a). This phenomenon is similar to the mixing process in the nanoprecipitation, where smaller and more

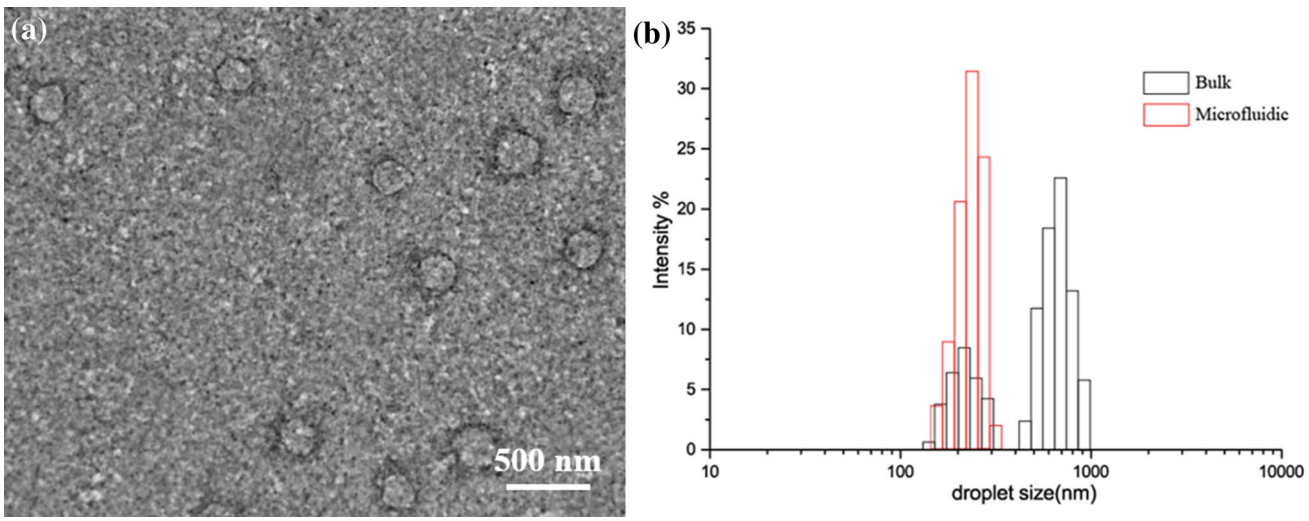

Fig. 2 **a** Transmission electron microscopy (TEM) images of PFOB nanodroplets produced by the Ouzo effect using the staggered herringbone mixer. The total flow rate was 2 ml/ml, the mixing ratio of organic versus aqueous phases was 1:4, and the organic phase consisted of 1 mg/ml lipid and 5 μl/ml PFOB in IPA. **b** Size distribution of the PFOB nanodroplets formed using the staggered herringbone mixer or by magnetic stirring in bulk

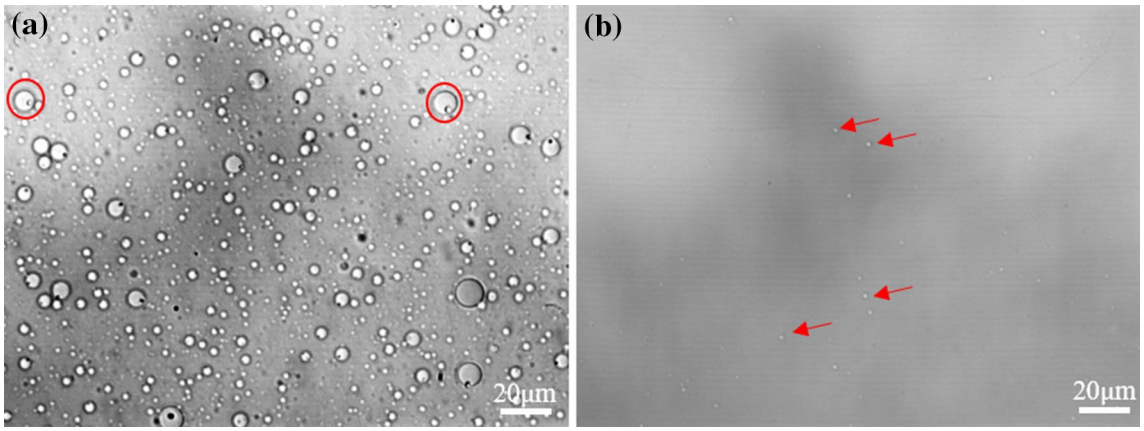

Fig. 3 Optical microscopy images of PFOB droplets obtained by mixing of 10 ul/ml PFOB in IPA and water at the organic: aqueous phase mixing ratio of 1:4. **a** PFOB droplets resulted from bulk mixing (i.e., magnetic stirring), red circles labeling the W/O/W double emulsion droplets; **b** PFOB droplets resulted from microfluidic mixing, red arrows indicating larger PFOB droplets

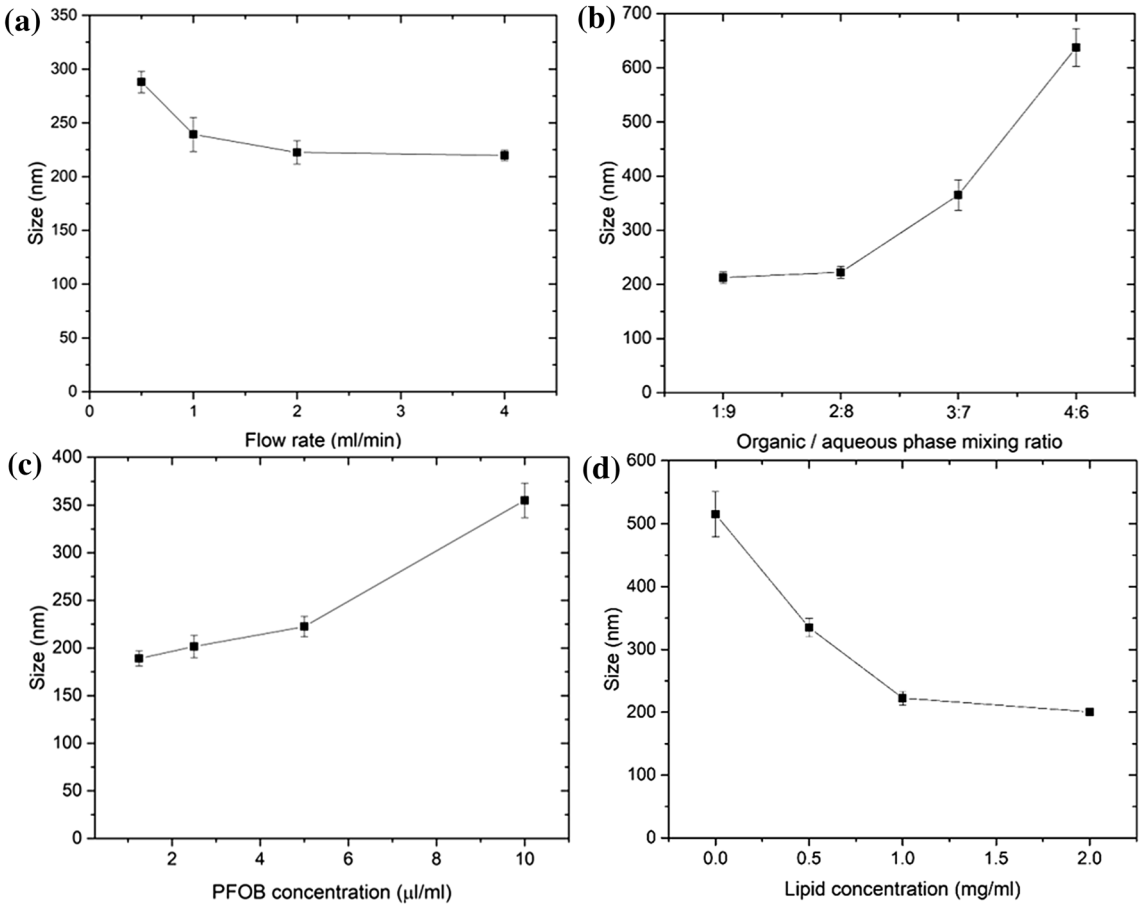

Fig. 4 The effects of the flow rate, mixing ratio, PFC concentration, and lipid concentration on the size of PFOB nanodroplets produced by the Ouzo effect using the staggered herringbone mixer. **a** Size of the PFOB nanodroplets decreased as the total flow rate (FR) increased. The mixing ratio of organic versus aqueous phases (MR) was 1:4 and the organic phase consisted of 1 mg/ml of lipid and 5 μl/ml of PFOB in IPA. **b** Size of the PFOB nanodroplets increased as the MR increased. FR = 2 ml/min and the organic phase consisted of 1 mg/ml of lipid and 5 μl/ml of PFOB in IPA. **c** Size of the PFOB nanodroplets increased as the PFOB concentration increased from 1.25 to 10 μl/ml and the lipid concentration increased from 0.25 to 2 mg/ml. FR and MR were kept at FR = 2 ml/min and MR = 1:4. **d** Size of the PFOB nanodroplets decreased as the lipid concentration increased. FR and MR were kept at FR = 2 ml/min and MR = 1:4, and PFOB was kept at 5 μl/ml in the organic phase

homogenous particles are produced when the particle formation is dominated by nucleation if mixing occurs faster than aggregation of polymers (Karnik et al. 2008). Figure 4b, c shows that increasing both MR and PFOB concentration in the organic phase resulted in larger PFOB nanodroplets, since higher PFOB concentration in the final mixture was determined from these two conditions, and the droplet diameter increased as the increase of oil fraction in the solvent (i.e., the amount of oil dissolved in the final mixed solution) by the Ouzo effect (Sitnikova et al. 2005; Vitale and Katz 2003). Furthermore, at a higher MR, the final IPA concentration was increased, leading to larger droplets due to the Ostwald ripening after complete mixing. Although droplets can be formed by the Ouzo effect without surfactants (Ganachaud and Katz 2005; Sitnikova et al. 2005; Vitale and Katz 2003), the employment of surfactants leads to smaller and stable nanodroplets by the Ouzo effect (Bouchemal et al. 2004; Saberi et al. 2013). We applied the lipids as the surfactants to stabilize the PFOB nanodroplets due to the excellent biocompatibility. Figure 4d reveals that the size of the PFOB nanodroplets decreased as the increase of lipid concentration. Because the hydrophilic end groups of the surfactants absorbed on the surface of nanodroplets, the surfactants helped prevent further absorption of free oil molecules to the nanodroplets and suppress following Ostwald ripening of the nanodroplets. We have also synthesized nanodroplets made of other PFC oils, e.g., PFH and PFCE. The total flow rate was kept at 2 ml/min, MR was 1:4, and the organic phase consisted of 1 mg/ml lipid and 5 µl/ml PFC. The results are summarized in Table 1. The PFOB nanodroplets are slightly smaller than other kinds of PFC, since PFOB has higher solubility in IPA leading to a lower PFC concentration in the final mixture and, therefore, smaller size of the resultant nanodroplets. Our nanoemulsification method greatly enhanced the throughput of nanodroplet production. The total flow rate could be up to 4 ml/min in our device and the corresponding PFC nanodroplet production rate was up to 0.48 ml/h (Table 2). The PFC nanodroplet production rate was calculated as the product of PFC concentration in IPA solution, MR and the total flow rate with assuming no loss of PFC nanodroplets in the purification process. The product rate has been increased by three orders of the magnitude, compared to the flow-focusing microfluidic devices at typical droplet generation rates of 0.1–10 KHz (Akbari et al. 2017) or even 1.3 MHz for 5.33×10^{-4} ml/h (Shim et al. 2013), estimated by assuming nanodroplet size of 300 nm in diameter. The comparison of droplet production methods is summarized in Table S1.

Table 1 Size, polydispersity index (PDI) of PFC nanodroplets (NDs) made of PFOB, PFH and PFCE, synthesized by the Ouzo effect using the staggered herringbone mixer

	Size (nm)	PDI
PFOB NDs	222.5 ± 10.7	0.08 ± 0.03
PFH NDs	248.8 ± 14.9	0.09 ± 0.02
PFCE NDs	259.9 ± 13.1	0.11 ± 0.02

Table 2 Nanodroplet production rate versus the total flow rate and the PFC concentration

Total flow rates (ml/min)	Nanodroplet production rate (ml/h)	
	PFC = 5 µl/ml	PFC = 10 µl/ml
2.0	0.12	0.24
4.0	0.24	0.48

3.2 Stability of PFC nanodroplets

The stability of PFC nanodroplets is crucial for shelf storage. We monitored the size variation of the prepared PFC nanodroplets (10 µl/ml) at 4 °C for 1 month. The mean diameter of the PFC nanodroplets increased less than 15% of their initial value, and the PFC nanodroplets with higher boiling points (i.e., PFOB, PFCE) were more stable than their counterparts (e.g., PFH), as shown in Fig. 5. The droplet growth was mainly attributed to the Ostwald ripening where the droplets grow at the cost of dissolution of small ones, which was also observed in the fluorinated stabilized PFC nanodroplets (Astafyeva et al. 2015).

3.3 Biocompatibility of PFC nanodroplets

PFC oils and lipids used for the preparation of PFC nanodroplets have been verified to be biocompatible by many others

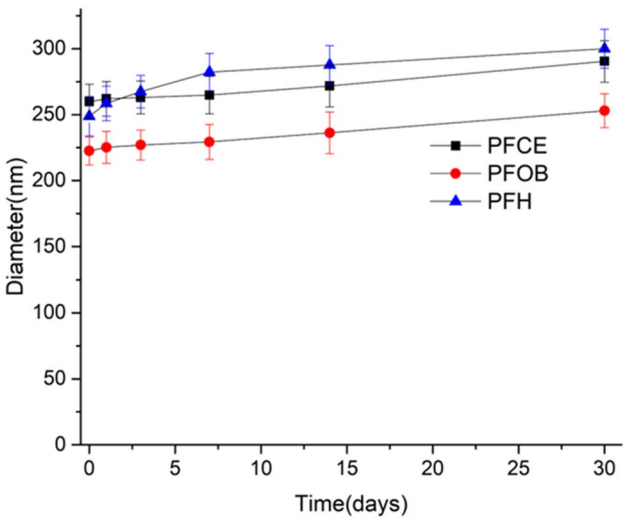

Fig. 5 Variations in the mean diameter of the prepared PFC nanodroplets stored at 4 °C over 30 days

(Leese et al. 2000; Lowe 1999); however, the organic solvent residue from the preparing process may be a potential threaten. Thus, we evaluated the cytotoxicity of the prepared PFC nanodroplets in cell cultures. Figure 6 plots the cell viability versus the concentration of the PFC nanodroplets in Hela cell culture medium solutions. We found no significant cytotoxicity below 8 μl/ml, which suggested that the prepared PFC nanodroplets were safe using typical doses (< 5 μl/ml) of the PFC nanodroplets for biomedical applications such as tumor imaging and drug delivery (Rapoport et al. 2011, 2009b).

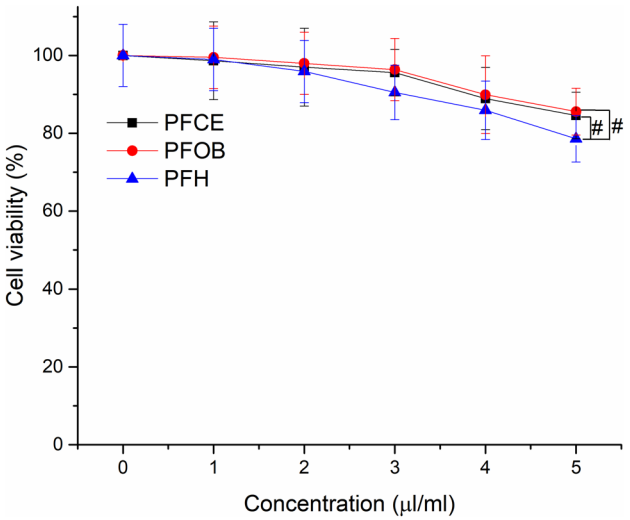

Fig. 6 In vitro cell viability versus the PFC nanodroplet concentration in the HeLa cell cultures and no statistically significant difference between different PFCs ($^{\#}p > 0.05$). The cell viability was measured after the Hela cells treated with PFC nanodroplets of different concentrations for 24 h

3.4 In vitro ultrasound imaging

PFC nanodroplets per se cannot effectively enhance ultrasound imaging due to their poor echogenicity (Ngo et al. 2000); therefore, the conversion of PFC nanodroplets to echogenic microbubbles in situ is required for PFC nanodroplets to function as ultrasound contrast agents. To prove the feasibility of the fabricated PFC nanodroplets as ultrasound contrast agents, we conducted acoustic activation tests of the PFC nanodroplets in the plastic Pasteur tubes loaded with the PAA gel. Before high-intensity ultrasound exposure, no bright spots appeared in the ultrasound images. After 15-s high-intensity ultrasound burst at an MI of 1.5, the bright spots appeared in the ultrasound images of the PFC nanodroplets, indicating the PFC nanodroplets had been successfully vaporized into highly echogenic gaseous microbubbles, as shown in Fig. 7a. And among the ultrasound images of the PFCE, PFOB and PFH nanodroplets, the PFH nanodroplets presented stronger signal, which implied more PFH nanodroplets were converted into microbubbles after the high-intensity ultrasound exposure. The signals of the PFC nanodroplets seemed to be related to their boiling point as PFH (b.p. 56 °C) has the lower boiling point than PFOB (b.p. 140–142 °C) and PFCE (b.p. 145 °C), which suggests that the PFC nanodroplets with a high boiling temperature

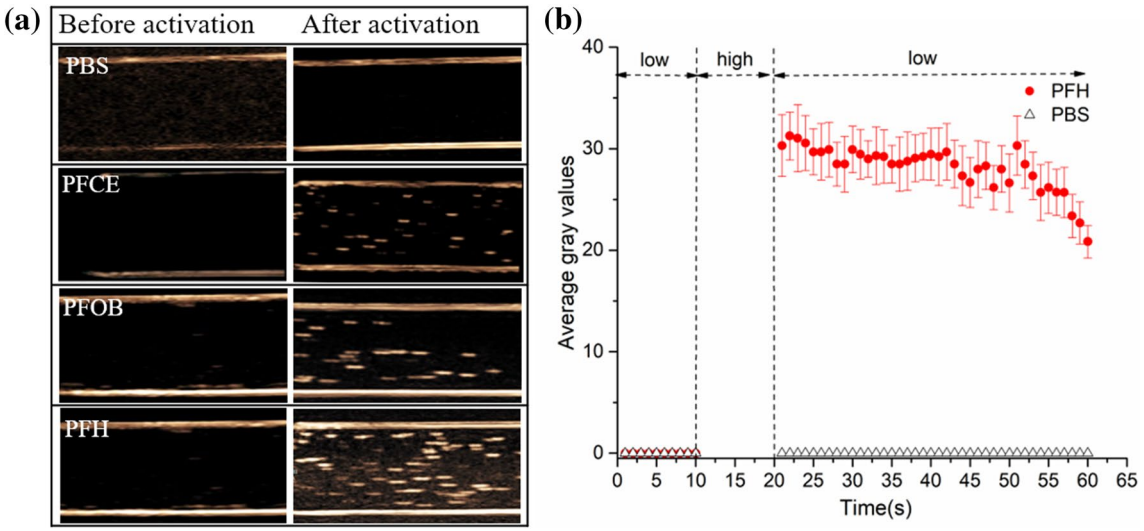

Fig. 7 In vitro ultrasound activation of the PFC nanodroplets embedded in the PAA gel phantoms. **a** Ultrasound images of PFCE, PFOB and PFH nanodroplets (at concentration of 5 μl/ml) in the PAA gel phantoms before/after 15-s high-intensity ultrasound exposure (MI at 1.5), and then the images were acquired at a frequency of 8 MHz and an MI of 0.2. PBS solution was used as a control. **b** Average gray values of time-series ultrasound images of the PFH nanodroplets and PBS control in the PAA gel phantoms. After the high-intensity ultrasound exposure, the ultrasound signal maintained for ~ 30 s and began to decline gradually

may have higher ADV thresholds (Rapoport et al. 2011). Therefore, the PFH nanodroplets with higher conversion efficiency are preferred for in vivo ultrasound imaging (Sheeran et al. 2012). And the PFOB and PFCE nanodroplets with good stability are favorably used for ultrasound ablation where the ultrasound with a higher intensity is allowed in these applications (Ma et al. 2014). Time-series ultrasound images of the PFH nanodroplets loaded in the gel phantom were analyzed with software Image J and the average gray values of the images representing the ultrasound signal intensity were recorded in time (Fig. 7b). After the high-intensity ultrasound exposure, the ultrasound signal maintained for ~ 30 s and started to decline gradually, which allowed adequate time for diagnosis at a clinically moderate level of MI. Apart from the boiling temperature of PFC, the size and size distribution of PFC nanodroplets also have a great impact on the ADV threshold (Kripfgans et al. 2004). Since the pressure inside droplets is inversely proportional to droplet size according to the Young–Laplace equation (Shpak et al. 2014) and smaller droplets have higher boiling temperatures than larger droplets based on the Antoine equation which implies the dependence of the vaporization temperature on the pressure (Rapoport et al. 2009a). Therefore, PFC nanodroplets with high monodispersity allows for delicate control of the vaporization process, due to their uniform response to ultrasound exposure, which may reduce the severe safety risk of gas embolism in the biomedical applications of PFC nanodroplets such as drug delivery, tumor imaging and ablation caused by the unwanted vaporization of polydisperse populated droplets.

4 Conclusions

We report a robust and high-throughput strategy for production of monodisperse PFC nanodroplets by the Ouzo effect using a staggered herringbone mixer. The size of the PFC nanodroplets can be tightly controlled from ~ 200 to ~ 700 nm in diameter by tuning operation parameters of the mixer and PFC/lipid concentration. And the throughput of nanodroplets production could be as high as 0.48 ml/h. The prepared PFC nanodroplets exhibited good stability and biocompatibility. The conversion of PFC nanodroplets to microbubbles has also been verified using a clinical ultrasound diagnostic system. Compared to droplet-based microfluidics, nanodroplet generation by the Ouzo effect using microfluidic mixers is easier to control and more robust in operation, and more importantly, can increase the production rate by approximately three orders of magnitude. We believe this nanoemulsification method offers a promise strategy to produce other functional nanoemulsions such as iodinated oil nanoemulsions as CT contrast agents.

Acknowledgements This work was financially supported by Research Grants Council of Hong Kong under General Research Fund (Grant no. 16206915) and Guangdong—Hong Kong Technology Cooperation Funding Scheme (Grant no. 2017A050506020).

Compliance with ethical standards

Conflict of interest There are no conflicts to declare.

References

Akbari S, Pirbodaghi T, Kamm RD, Hammond PT (2017) A versatile microfluidic device for high throughput production of microparticles and cell microencapsulation. Lab Chip 17:2067–2075

Aschenbrenner E, Bley K, Koynov K, Makowski M, Kappl M, Landfester K, Weiss CK (2013) Using the polymeric ouzo effect for the preparation of polysaccharide-based nanoparticles. Langmuir 29:8845–8855

Astafyeva K et al (2015) Perfluorocarbon nanodroplets stabilized by fluorinated surfactants: characterization and potentiality as theranostic agents. J Mater Chem B 3:2892–2907

Beck-Broichsitter M, Nicolas J, Couvreur P (2015) Solvent selection causes remarkable shifts of the "Ouzo region" for poly (lactide-*co*-glycolide) nanoparticles prepared by nanoprecipitation. Nanoscale 7:9215–9221

Bouchemal K, Briançon S, Perrier E, Fessi H (2004) Nano-emulsion formulation using spontaneous emulsification: solvent, oil and surfactant optimisation. Int J Pharmaceut 280:241–251

Díaz-López R, Tsapis N, Fattal E (2010a) Liquid perfluorocarbons as contrast agents for ultrasonography and 19F-MRI. Pharmaceut Res 27:1

Díaz-López R et al (2010b) The performance of PEGylated nanocapsules of perfluorooctyl bromide as an ultrasound contrast agent. Biomaterials 31:1723–1731

Ganachaud F, Katz JL (2005) Nanoparticles and nanocapsules created using the ouzo effect: spontaneous emulsification as an alternative to ultrasonic and high-shear devices. ChemPhysChem 6:209–216

Haase MF, Stebe KJ, Lee D (2015) Continuous fabrication of hierarchical and asymmetric bijel microparticles, fibers, and membranes by solvent transfer-induced phase separation (STRIPS). Adv Mater 27:7065–7071

Hettiarachchi K, Talu E, Longo ML, Dayton PA, Lee AP (2007) On-chip generation of microbubbles as a practical technology for manufacturing contrast agents for ultrasonic imaging. Lab Chip 7:463–468

Jahn A, Stavis SM, Hong JS, Vreeland WN, DeVoe DL, Gaitan M (2010) Microfluidic mixing and the formation of nanoscale lipid vesicles. ACS Nano 4:2077–2087

Jeong W-C et al (2012) Controlled generation of submicron emulsion droplets via highly stable tip-streaming mode in microfluidic devices. Lab Chip 12:1446–1453

Kaneda MM, Caruthers S, Lanza GM, Wickline SA (2009) Perfluorocarbon nanoemulsions for quantitative molecular imaging and targeted therapeutics. Ann Biomed Eng 37:1922–1933

Karnik R et al (2008) Microfluidic platform for controlled synthesis of polymeric nanoparticles. Nano Lett 8:2906–2912

Klossek ML, Touraud D, Zemb T, Kunz W (2012) Structure and solubility in surfactant-free. Microemulsions ChemPhysChem 13:4116–4119

Koroleva MY, Yurtov EVe (2012) Nanoemulsions: the properties, methods of preparation and promising applications. Russ Chem Rev 81:21–43

Kotta S, Khan AW, Pramod K, Ansari SH, Sharma RK, Ali J (2012) Exploring oral nanoemulsions for bioavailability enhancement of poorly water-soluble drugs. Expert Opin Drug Deliv 9:585–598

Kripfgans OD, Fabiilli ML, Carson PL, Fowlkes JB (2004) On the acoustic vaporization of micrometer-sized droplets. J Acoust Soc Am 116:272–281

Leese PT, Noveck RJ, Shorr JS, Woods CM, Flaim KE, Keipert PE (2000) Randomized safety studies of intravenous perflubron emulsion. I. Effects on coagulation function in healthy volunteers. Anesth Anal 91:804–811

Lepeltier E, Bourgaux C, Couvreur P (2014) Nanoprecipitation and the "Ouzo effect": application to drug delivery devices. Adv Drug Deliv Rev 71:86–97

Li DS, Yoon SJ, Pelivanov I, Frenz M, O'Donnell M, Pozzo LD (2017) Polypyrrole-coated perfluorocarbon nanoemulsions as a sono-photoacoustic contrast. Agent Nano Lett 17:6184–6194

Lim J-M et al (2014) Ultra-high throughput synthesis of nanoparticles with homogeneous size distribution using a coaxial turbulent jet mixer. ACS Nano 8:6056–6065

Lowe K (1999) Perfluorinated blood substitutes and artificial oxygen carriers. Blood Rev 13:171–184

Lu Z, Schaarsberg MHK, Zhu X, Yeo LY, Lohse D, Zhang X (2017) Universal nanodroplet branches from confining the Ouzo effect. Proc Natl Acad Sci 114:10332–10337

Ma M et al (2014) A drug–perfluorocarbon nanoemulsion with an ultrathin silica coating for the synergistic effect of chemotherapy and ablation by high-intensity focused ultrasound. Adv Mater 26:7378–7385

Martz TD, Sheeran PS, Bardin D, Lee AP, Dayton PA (2011) Precision manufacture of phase-change perfluorocarbon droplets using microfluidics. Ultrasound Med Biol 37:1952–1957

Martz TD, Bardin D, Sheeran PS, Lee AP, Dayton PA (2012) Microfluidic generation of acoustically active nanodroplets. Small 8:1876–1879

Ngo FC et al (2000) Evaluation of liquid perfluorocarbon nanoparticles as a blood pool contrast agent utilizing power Doppler harmonic imaging. In: Ultrasonics Symposium, 2000 IEEE, IEEE, pp 1931–1934

Perera RH, Hernandez C, Zhou H, Kota P, Burke A, Exner AA (2015) Ultrasound imaging beyond the vasculature with new generation contrast agents. Wiley Interdisciplinary Reviews. Nanomed Nanobiotechnol 7:593–608

Rapoport N, Gao Z, Kennedy A (2007) Multifunctional nanoparticles for combining ultrasonic tumor imaging and targeted chemotherapy. J Natl Cancer Inst 99:1095–1106

Rapoport NY, Efros AL, Christensen DA, Kennedy AM, Nam K-H (2009a) Microbubble generation in phase-shift nanoemulsions used as anticancer drug carriers. Bubble Sci Eng Technol 1:31–39

Rapoport NY, Kennedy AM, Shea JE, Scaife CL, Nam K-H (2009b) Controlled and targeted tumor chemotherapy by ultrasound-activated nanoemulsions/microbubbles. J Control Rel 138:268–276

Rapoport N et al (2011) Ultrasound-mediated tumor imaging and nanotherapy using drug loaded, block copolymer stabilized perfluorocarbon nanoemulsions. J Control Rel 153:4–15

Reznik N, Williams R, Burns PN (2011) Investigation of vaporized submicron perfluorocarbon droplets as an ultrasound contrast agent. Ultrasound Med Biol 37:1271–1279

Saberi AH, Fang Y, McClements DJ (2013) Fabrication of vitamin E-enriched nanoemulsions: factors affecting particle size using spontaneous emulsification. J Colloid Interface Sci 391:95–102

Segers T, de Rond L, de Jong N, Borden M, Versluis M (2016) Stability of monodisperse phospholipid-coated microbubbles formed by flow-focusing at high production rates. Langmuir 32:3937–3944

Seo M, Matsuura N (2014) Direct incorporation of lipophilic nanoparticles into monodisperse perfluorocarbon nanodroplets via solvent dissolution from microfluidic-generated precursor microdroplets. Langmuir 30:12465–12473

Seo M, Williams R, Matsuura N (2015) Size reduction of cosolvent-infused microbubbles to form acoustically responsive monodisperse perfluorocarbon nanodroplets. Lab Chip 15:3581–3590

Sheeran PS, Luois SH, Mullin LB, Matsunaga TO, Dayton PA (2012) Design of ultrasonically-activatable nanoparticles using low boiling point perfluorocarbons. Biomaterials 33:3262–3269

Shim J-u et al (2013) Ultrarapid generation of femtoliter microfluidic droplets for single-molecule-counting immunoassays. 7:5955–5964

Shpak O, Verweij M, Vos HJ, de Jong N, Lohse D, Versluis M (2014) Acoustic droplet vaporization is initiated by superharmonic focusing. Proc Natl Acad Sci 111:1697–1702

Shui L, van den Berg A, Eijkel JC (2011) Scalable attoliter monodisperse droplet formation using multiphase nano-microfluidics. Microfluid Nanofluid 11:87–92

Sitnikova NL, Sprik R, Wegdam G, Eiser E (2005) Spontaneously formed trans-anethol/water/alcohol emulsions mechanism of formation stability. Langmuir 21:7083–7089

Stroock AD, Dertinger SK, Ajdari A, Mezić I, Stone HA, Whitesides GM (2002) Chaotic mixer for microchannels. Science 295:647–651

Talu E, Lozano MM, Powell RL, Dayton PA, Longo ML (2006) Long-term stability by lipid coating monodisperse microbubbles formed by a flow-focusing device. Langmuir 22:9487–9490

Tan H, Diddens C, Lv P, Kuerten JG, Zhang X, Lohse D (2016) Evaporation-triggered microdroplet nucleation and the four life phases of an evaporating Ouzo drop. Proc Natl Acad Sci 113:8642–8647

Vitale SA, Katz JL (2003) Liquid droplet dispersions formed by homogeneous liquid–liquid nucleation:"The ouzo effect". Langmuir 19:4105–4110

Xu X et al (2017) Microfluidic production of nanoscale perfluorocarbon droplets as liquid contrast agents for ultrasound imaging. Lab Chip

Yan X et al (2014) Simple but precise engineering of functional nanocapsules through nanoprecipitation. Angew Chem Int Ed 53:6910–6913

Zhang Q, Liu X, Liu D, Gai H (2014) Ultra-small droplet generation via volatile component evaporation. Lab Chip 14:1395–1400

Zhang X, Lu Z, Tan H, Bao L, He Y, Sun C, Lohse D (2015) Formation of surface nanodroplets under controlled flow conditions Proc Natl Acad Sci 112:9253–9257